HELLENIC CENTRE FOR MARINE RESEARCH

Mediterranean Marine Science

VOLUME 14 • Number 3 • (special issue)

Temperature and salinity variability in the Greek Seas based on POSEIDON stations time series: preliminary results

D. VELAORAS, D. KASSIS, L. PERIVOLIOTIS, P. PAGONIS, A. HONDRONASIOS, K. NITTIS

Temperature and salinity variability in the Greek Seas based on POSEIDON stations time series: preliminary results

D. VELAORAS, D. KASSIS, L. PERIVOLIOTIS, P. PAGONIS, A. HONDRONASIOS and K. NITTIS

Hellenic Centre for Marine Research, Institute of Oceanography, P.O. Box 712, 19013 Anavissos, Greece

Corresponding author: dvelaoras@hcmr.gr

Abstract

Temperature and salinity time series provided by three POSEIDON monitoring stations (buoys) are examined in order to study the seasonal and interannual variability of the water mass characteristics. The sites at Athos (North Aegean Sea), E1M3A (Central Cretan Sea) and Pylos (Eastern Ionian Sea) were chosen, as these buoys provide measurements at various depths, while they represent 3 major basins respectively. The study of the T and S characteristics reveals important seasonal changes and highlights the particular characteristics of each basin. Dense water production in the Northern Aegean is found to be hindered by the presence of the surface Black Sea Water (BSW) mass. On the other hand, the intermediate water mass in the Cretan Sea is shown to be ventilated during the winter season. A significant temperature and salinity increase has been monitored over both the Central Cretan and Eastern Ionian Seas starting from the middle of 2008 and 2009 respectively. This could possibly be attributed to changes in the intermediate water masses of the Eastern Mediterranean, without ruling out the possibility of water mass exchanges between the two basins.

Keywords: Operational Oceanography, Aegean Sea, Eastern Mediterranean, intermediate water mass formation.

Introduction

General water mass characteristics

The Aegean Sea consists of two major basins: 1) The North – Central Aegean basin bounded to the north and west by the Greek mainland and to the south by the Cyclades Islands complex, and 2) the South Aegean basin (Cretan Sea) south of the Cyclades and up to the island of Crete.

A major characteristic of the North Aegean surface circulation is the intrusion through the Dardanelles Straits of a low salinity surface water mass of Black Sea origin called Black Sea Water (BSW). After entering the Aegean Sea, BSW fills the northern part of the basin up to about 40 m depth and following a cyclonic path moves to the southwest reaching the western Cyclades region (Zodiatis, 1994; Zodiatis *et al*., 1996; Zervakis *et al*., 2005). BSW salinity at the Dardanelles exit is as low as 23-28 psu (Oğuz & Sur, 1989; Ünlüata *et al*., 1990), which makes this water mass less dense than the surrounding more saline Aegean surface masses. During its southward course, BSW gradually increases its salinity by mixing with Aegean surface waters. BSW is traced in the western part of the South Aegean up to the West Cretan Straits (Theocharis *et al*., 1993, 1999).

Another surface mass, which appears in the North as well as in the South Aegean Sea, is a water mass of Levantine origin entering the South Aegean through the East Cretan Straits, called Levantine Surface Water (LSW). It carries highly saline water masses with salinities reaching values of more than 39.20 psu during the summer period (Theocharis *et al*., 1993, 1999). After its entrance in the Aegean, LSW moves westwards feeding the Cretan Sea while a second branch moves northwards entering the Central Aegean reaching up to the North Aegean basins (Zodiatis, 1994; Velaoras & Lascaratos, 2010).

In the South Aegean, a surface/subsurface water mass of Atlantic origin, namely Atlantic Water (AW) can be observed entering mainly through the West Cretan Straits (Zodiatis, 1991; Theocharis *et al*., 1993, 1999) but it has also been traced in the Eastern (Kassos) Straits (Theocharis *et al*., 1999). It is traced as a local salinity minimum (38.5 – 38.9 psu) moving from the Straits to the centre of the basin at depths of 30 – 100 dbars. Its presence is also evident in the Ionian Sea as a surface/subsurface salinity minimum (Kress *et al*., 2003).

In the intermediate layer below the BSW, LSW and AW masses, a warm and saline water mass is found in both the Aegean and the Ionian Seas. This is Levantine Intermediate Water (LIW) formed in the Levantine Sea during winter. After its formation, LIW moves westwards slowly reducing its salt and heat content. LIW is traced in the intermediate layer as a local salinity maximum occupying the Eastern Mediterranean (Wüst, 1961). LIW

Medit. Mar. Sci., SPECIAL ISSUE, 2013, 5-18

5

enters the South Aegean Sea through the Cretan Straits (Theocharis *et al.*, 1993; Zodiatis, 1994; Astraldi *et al.*, 1999) bifurcating into two branches. The first one fills the Cretan Sea while the second one moves towards the northern Aegean basin. LIW masses alter their characteristics in both basins. In the Northern Aegean, LIW mixes with intermediate masses locally produced during winter thus increasing its density (Gertman *et al.*, 2006). The Cretan Sea itself produces intermediate water masses called Cretan Intermediate Water (CIW) with characteristics very close to those of LIW, with the former being slightly denser (Theocharis *et al.*, 1998; Astraldi *et al.*, 1999). CIW has been observed outflowing in discrete pulses from the Cretan Straits to the Eastern Mediterranean where it stabilizes beneath the LIW layer as an intermediate water mass slightly denser than LIW (Schlitzer *et al.*, 1991; Malanotte-Rizzoli *et al.*, 1997).

The POSEIDON system and data

The POSEIDON-II (2005-2008) system significantly upgraded the monitoring and forecasting capability of the original POSEIDON system, which has been operating in the Greek Seas since 2000 (Soukissian *et al.*, 2002; Nittis *et al.*, 2002; Petihakis *et al.*, 2009; www.poseidon.hcmr.gr). The upgrade included the addition of two new multi-parametric monitoring stations (buoys) in the Central Cretan Sea (E1M3A) and in the Eastern Ionian Sea (Pylos). In this paper, preliminary results of temperature and salinity measurements are presented for the aforementioned locations. Buoy positions are shown in Figure 1.

The station locations represent three basins with different water mass characteristics, which on the other hand interact with each other, as shown in section 1.1. Table 1 presents the type and depth of the installed temperature and salinity sensors at each buoy. In this work, only time series that do not contain significant discontinuities were used, according to Table 2. Moored buoys were regularly uplifted and maintained at 6–8 month intervals. Sensors were replaced by newly calibrated ones in every deployment.

Surface salinity time series are not presented in the following figures, as surface salinity sensors are very
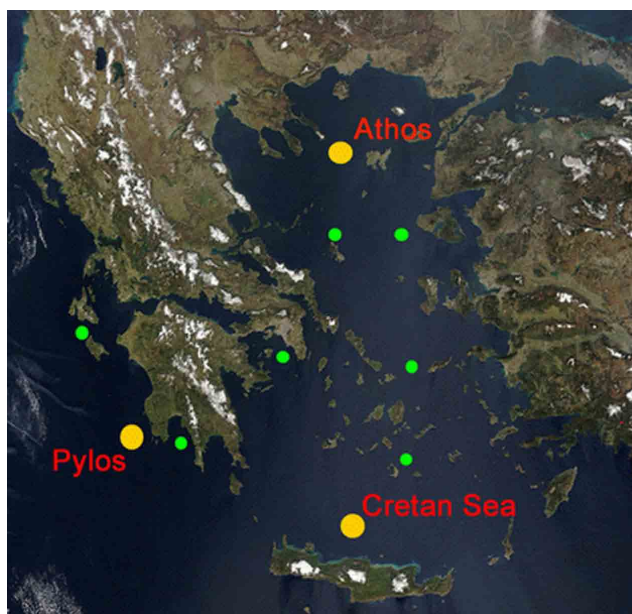
Fig. 1: Athos, Cretan Sea (E1M3A) and Pylos monitoring stations positions.

sensitive to biofouling and consequently surface salinity values are not reliable. Extreme values, spikes, and obviously wrong values due to sensor malfunction were removed from the dataset, following the MyOcean in-situ quality control standards (http://catalogue.myocean.eu.org/static/resources/user_manual/myocean/QUID_INSITU_TS_OBSERVATIONS-v1.0.pdf). Potential temperature (θ) and potential density (σ_θ) values were derived according to Unesco (1983) algorithms. Potential density was produced only by valid pairs of in-situ T and S. As salinity values are needed to produce θ values and since surface salinities are not used, in-situ T values are used for the surface θ time series. This is considered acceptable since θ and in-situ T do not differ substantially at 1m depth (surface). Finally, all time series (sampled at 3h intervals, 8 times daily in total) were treated with a low-pass Butterworth filter in order to remove high frequency (<5 days) signals.

Table 1. Temperature and Salinity sensor models and deployment depths for the Athos, Cretan Sea (E1M3A) and Pylos monitoring stations.

| Monitoring Position	T and S monitoring depths (m)	Sensor type
Athos	Surface, 20, 50, 75, 100	Aanderaa 3919A (Surface) Seabird 37 IM C-T (20-100 m)
Cretan Sea (E1M3A)	Surface, 20, 50, 75, 100, 250, 400, 600, 1000	Seabird SIP (Surface) Seabird 16plus-IMP C-T (20-100 m) Seabird 37 IM C-T (250-1000 m)
Pylos	Surface, 20, 50, 75, 100, 250, 400, 500	Aanderaa 3919A or Seabird SIP (Surface) Seabird 37 IM C-T (20-500 m)

6

Medit. Mar. Sci., SPECIAL ISSUE, 2013, 5-18

Table 2. Monitoring periods for the Athos, Cretan Sea (E1M3A) and Pylos monitoring stations.

Monitoring Position	Time Period
Athos	January 2008 – October 2010
Cretan Sea (E1M3A)	May 2007 – January 2009
Pylos	January 2008 – January 2011

Θ, S, and σθ time series

North Aegean Sea (Athos)

Figures 2, 3, and 4 present time series of θ, S and σθ at Athos station for a period starting in January 2008 up to October 2010. Θ is shown for 1, 20, 50, 75 and 100 m depths, while there are no surface values for S. Consequently, σθ has been derived from valid t and S pairs only.
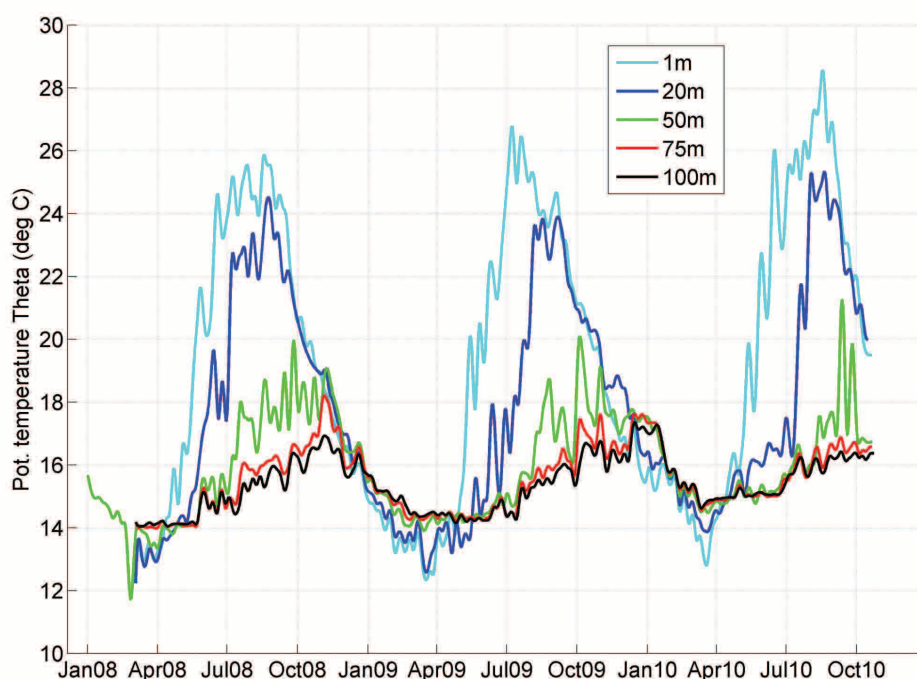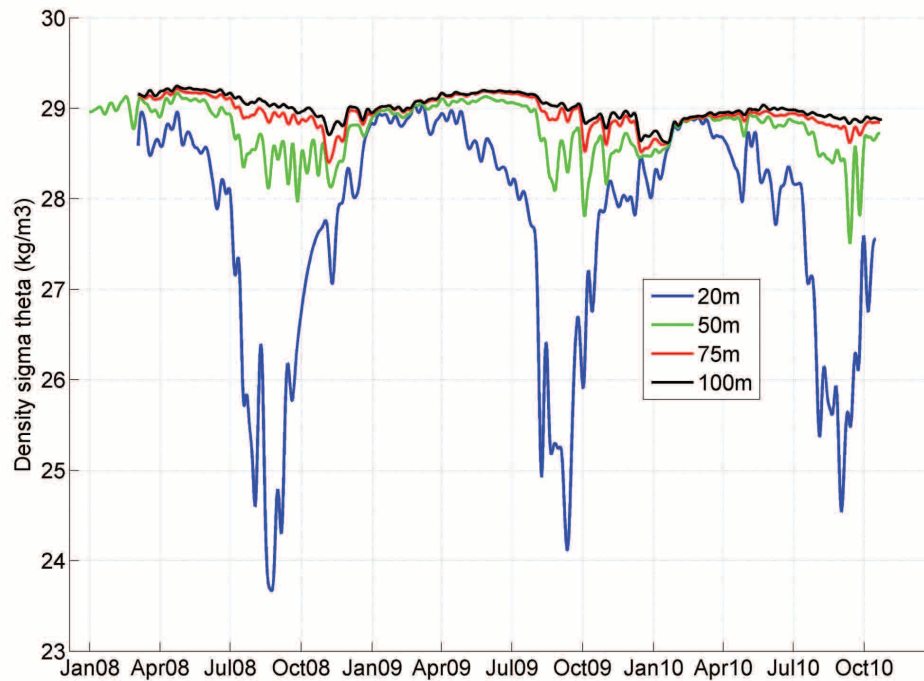

Fig. 2: Athos station. Time series of potential temperature (θ) at 1, 20, 50, 75 and 100 m depth (January 2008–October 2010).
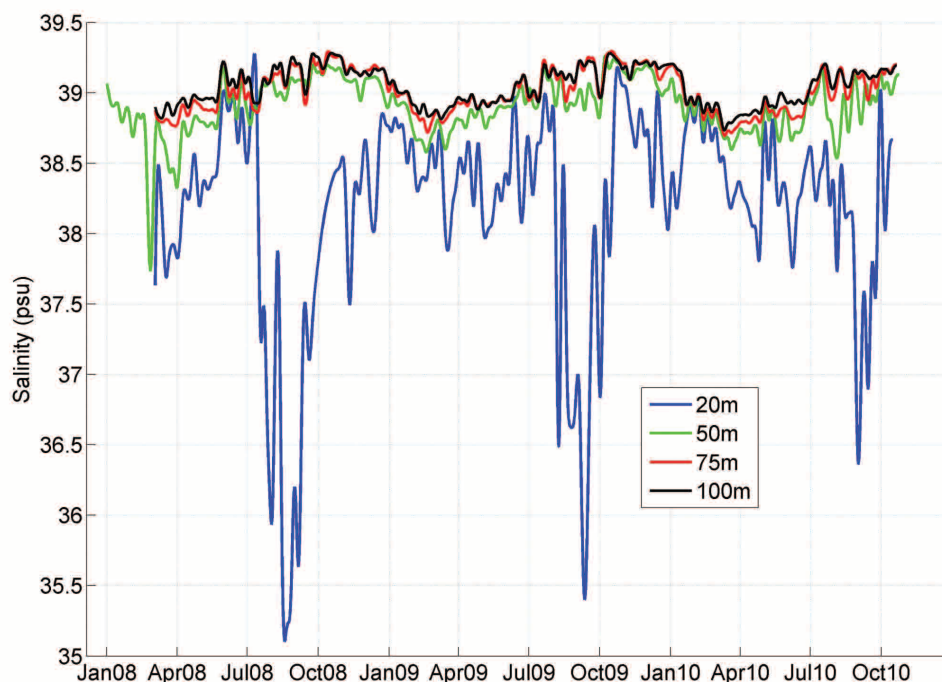
Fig. 3: Athos station. Time series of Salinity (θ) at 20, 50, 75 and 100 m depth (January 2008–October 2010).

Medit. Mar. Sci., SPECIAL ISSUE, 2013, 5-18

7

Fig. 4: Athos station. Time series of potential density (σ_θ) at 20, 50, 75 and 100 m depth (January 2008–October 2010).

Surface layer

Seasonal variability is prominent in all figures. Due to surface heating, the thermocline gradually develops from May each year and peaks during summer. The water column gradually looses heat starting in early autumn and from January to early spring it finally becomes homogenized (as far as densities are concerned). Homogenization is fully developed for the upper 100 m. Although no data is available for the area below 100 m in depth, it can be assumed that in the particular area and for the particular time period, winter homogenization should not have penetrated far below the first 100 m layer, as densities in this surface layer during the peak of homogenization do not in any case exceed 29 kg/m³. This means that density in the first 100 m is less than the density of the underlying intermediate water masses, which is greater than 29 kg/m³ (Velaoras & Lascaratos, 2010; Vervatis *et al.*, 2011). The results show that a deep-water formation episode in the Athos area is unlikely to have occurred during this particular time period. This of course cannot rule out the possibility of deep-water formation in some other area of the Northern Aegean, either in shelf areas or in the open sea (Georgopoulos *et al.*, 1992; Theocharis & Georgopoulos, 1993; Gertman *et al.*, 2006).

It is of particular interest that during the winter period while temperature values at the surface and 20 m deep are significantly lower than those of the underlying layers (Fig. 2), this does not lead to instability due to the low salinity values of the surface layer. The low surface salinity relates to the presence of BSW, which reaches the Athos area as a well-defined brackish surface water mass

(Zodiatis, 1994). The presence of low salinity BSW at the surface, hinders the dense water formation ability of the Northern Aegean, because this surface layer during cold winter events can lose significant amounts of buoyancy, without becoming dense enough to form deep waters (Zervakis *et al.*, 2000)

According to Zodiatis *et al.* (1996), the depth of the BSW influence does not exceed ~50 m. Surface salinities (20 m) reach a minimum of 35.2 – 36.7 psu during the summer period, due to the enhanced BSW intrusion in the North Aegean, which reaches its maximum during the same period (Zodiatis, 1994). This local salinity minimum appears to be reduced during the 2010 summer period when surface masses are more saline than in the summer of 2008 and 2009. This can be attributed either to interannual variations in the quantity or salinity of the inflowing BSW or to local circulation patterns at the Athos station area, which deflect the BSW course (Zervakis *et al.*, 2000; Velaoras & Lascaratos, 2010).
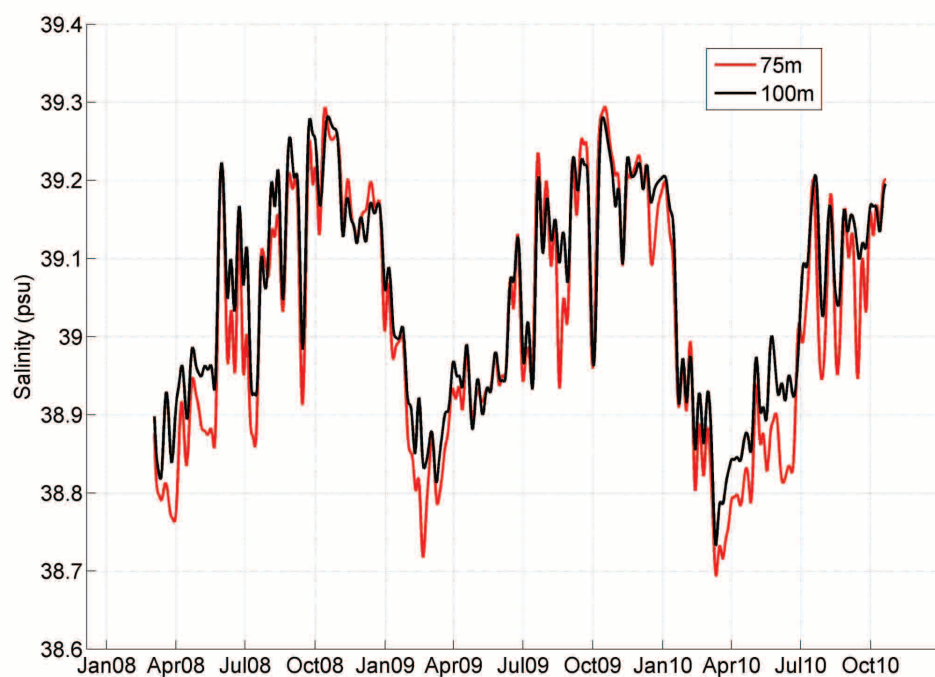
Subsurface/Intermediate layer

Figures 5, 6 and 7 present θ, S and σ_θ time series at the Athos station restricted to depths of 75 and 100 m.

Although the 100 m depth is not at the core of the intermediate layer in the North Aegean, it can be assumed that it is the upper limit of this layer (Velaoras & Lascaratos, 2010); thus, any changes in the characteristics of the 100 m layer can be linked to respective changes of intermediate layer characteristics. As a result, the salinity increase observed after the end of winter and up to the end of autumn is followed by an increase in temperature

Fig. 5: Athos station. Time series of potential temperature (θ) at 75 and 100m depth (January 2008–October 2010).
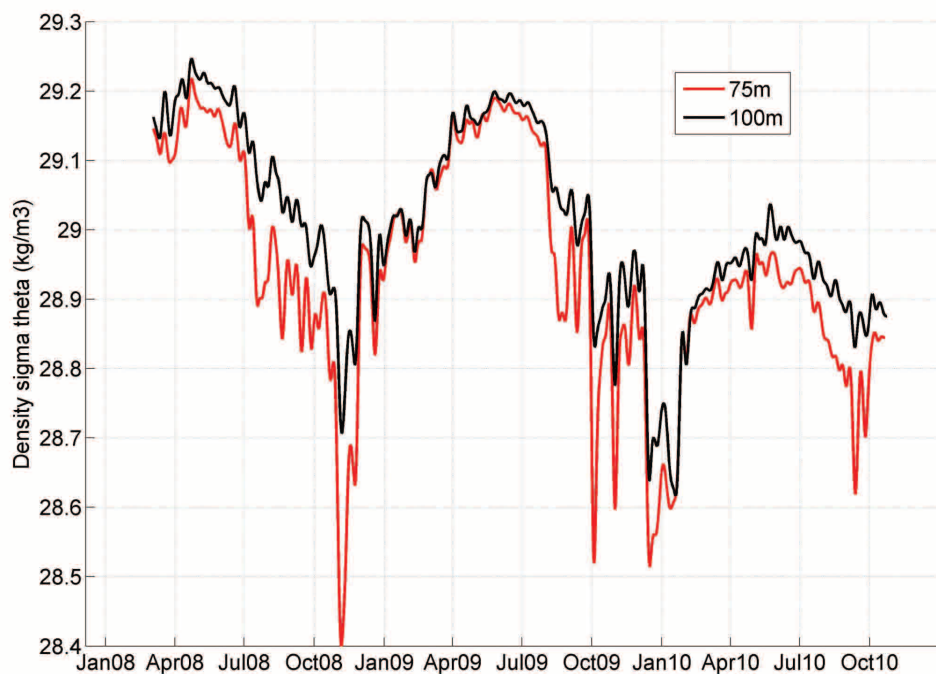

Fig. 6: Athos station. Time series of salinity at 75 and 100 m depth (January 2008–October 2010).

starting at the end of spring up to the beginning of winter. Moreover, during the summer season when the salinity of the intermediate layer increases, surface salinity decreases significantly as shown in Figure 3. This decoupling between surface and intermediate masses is linked with the cessation of winter homogenization. During this period, the intermediate layer is fed with a mixture of intermediate masses locally produced in the Central Aegean during winter (Gertman *et al*., 2006; Vervatis *et al*.,

2011) and of LIW masses, which enter the North Aegean through the South Aegean, which in turn communicates with the Levantine Sea through the East Cretan system (Zodiatis, 1994; Zervakis *et al*., 2000; Velaoras & Lascaratos, 2005).

Salinity at 100 m depth exceeds 39.2 psu during the summer period, while minimum values under winter homogenization are about 38.8 psu. Respective values for θ are maximum >17 °C and minimum 14 – 14.6 °C.

Medit. Mar. Sci., SPECIAL ISSUE, 2013, 5-18

9

Fig. 7: Athos station. Time series of potential density (σ_θ) at 20, 50, 75 and 100 m depth (January 2008–October 2010).

Maximum σ_θ at 100 m appears at the end of spring – early summer, and reaches 29.20 kg/m³ in 2008 and 2009 (which is about 0.2 kg/m³ greater than the value observed in winter). The density maximum is mainly temperature dependent and to a lesser extent salinity dependent. Thus, in 2010 (in comparison with 2008-9), the 0.5-1 ^{0}C temperature increase led to σ_θ values that did not exceed 29 kg/m³. This reduced density observed in 2010 is clearly shown in Figure 8 - density by depth evolution.

Central Cretan Sea (E1M3A)

Data from the Central Cretan Sea monitoring buoy for the period from May 2007 to January 2009 are presented in this section. Unfortunately, the Cretan and Athos time series have limited time overlapping, a fact that undermines their joint study. The values are obtained at 1, 20, 50, 75, 100, 250, 400, 600 and 1000 m for temperature and 20, 50, 75, 100, 250, 400, 600 and 1000 m for salinity as, once again, the surface salinity sensor suffers from
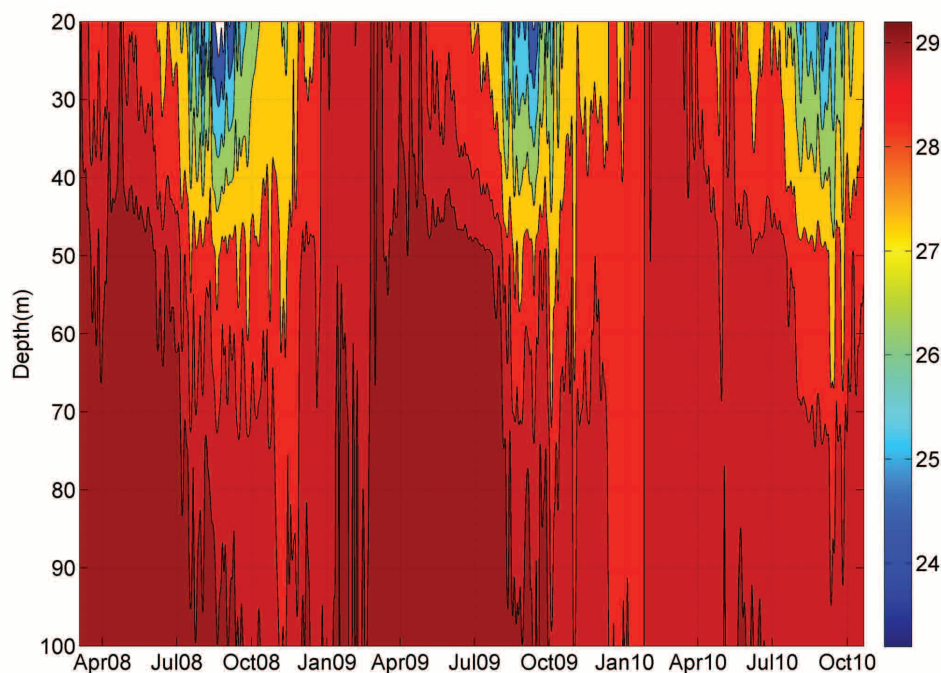

Fig. 8: Athos station. Potential density (σ_θ) by depth evolution (January 2008–October 2010).

10

Medit. Mar. Sci., SPECIAL ISSUE, 2013, 5-18

biofouling. Again, σ_θ has been derived from valid t and S pairs only. θ, S and σ_θ time series are presented in Figures 9, 10 and 11. Figure 10 presents salinity by depth evolution instead of salinity time series at discrete depths as the latter was hardly readable.

Surface layer

Strong seasonal variability is evident in these figures.

The seasonal thermocline starts developing in April and peaks at the end of the summer season. The slow erosion of the thermocline starts in mid-autumn and the water column gradually becomes homogenized. Homogenization reaches a peak during March and occupies the first 250 m without affecting the 400 m depth. It is thus confirmed that during the 2008 winter period there was intermediate water production in the Central Cretan Sea.
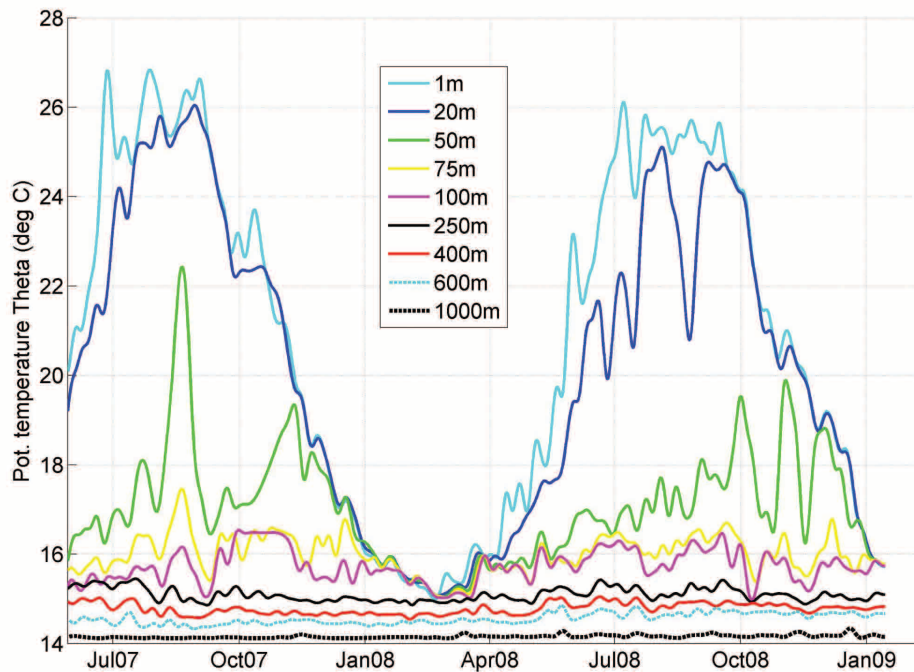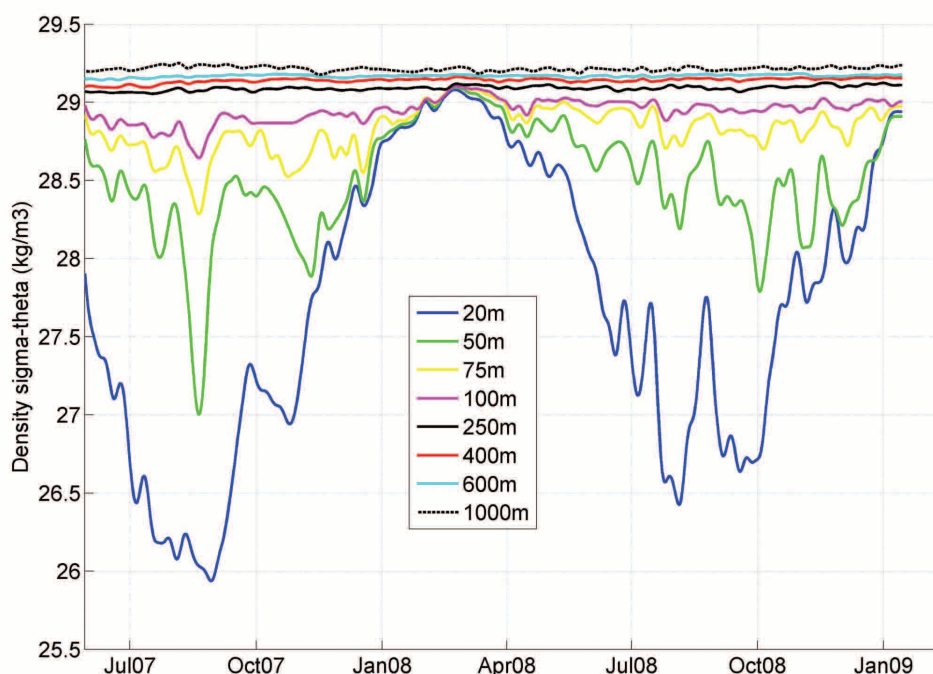

Fig. 9: Cretan Sea (E1M3A) station. Time series of potential temperature (θ) at 1, 20, 50, 75, 100,250, 400, 600 and 1000 m depth (May 2007–January 2009).
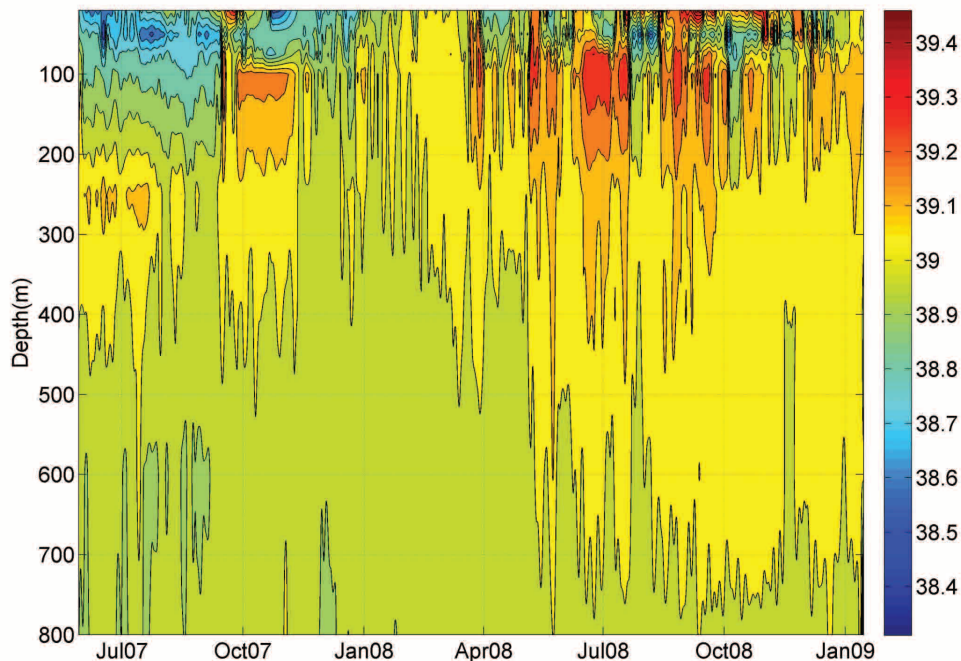
Fig. 10: Cretan Sea (E1M3A) station. Salinity by depth evolution (May 2007–January 2009).

Fig. 11: Cretan Sea (E1M3A) station. Time series of potential density (σ_θ) at 20, 50, 75, 100, 250, 400, 600 and 1000 m depth (May 2007–January 2009).

Intermediate water formation in the Cretan Sea has been observed in several cases (e.g. Georgopoulos *et al*., 1989; Roether *et al*., 1998) and it is a rather typical occurrence. During the peak of vertical convective mixing, σ_θ density in the 0-250 m layer is about 29.08-29.12 kg/m³, while θ and S values are 14.9-15.1 ⁰C and 39-39.06 psu respectively. According to the literature (Astraldi *et al*., 1999; Theocharis *et al*., 1998) these values correspond to CIW.

In Figure 10, which shows the salinity by depth evolution, the following distinct masses can be observed:

a) A low salinity surface/sub-surface water mass. Salinity values of about 38.5 – 38.9 psu point to either AW, which enters the Cretan Sea through the Cretan straits system (Theocharis *et al*., 1993, 1999) or to BSW reaching the area from the north Aegean through the western part of the south Aegean (Zodiatis, 1993). The low salinity core is found at a depth of about 50 m.

b) A high salinity surface/sub-surface water mass. This is LSW, which enters the Cretan Sea through the East Cretan straits system (Theocharis *et al*., 1993, 1999) and carries highly saline water masses with salinities reaching values of more than 39.20 psu during the summer period.

In the same Figure 10, an alternating presence of BSW/AW and LSW can be observed, which must be linked with local circulation features. The identification of these masses is much easier during summer as in winter the water column becomes homogenized at the BSW/AW/LSW horizons.

Intermediate layer

θ, S and σ_θ in 250 and 400 m time series are presented in Figures 12, 13 and 14. Figure 13 reveals a salin-ity increase in the intermediate layer starting from early 2008. Between October 2007 and October 2008 salinity at 400 m is increased by 0.06 psu, while the temperature increase is about 0.1 – 0.2 ⁰C. A slight (0.02 kg/m³) increase in the density of the intermediate layer is observed due to the salinity and temperature variations. The dominant characteristic of this variation (i.e. the salinity increase) could be attributed to the altered salinity values of the LIW masses that entered the Central Cretan Sea through the East Cretan Straits.

Finally, the time series at the depth of 1000 m reveal nearly constant values of $\theta \sim 14.15$ ⁰C, $S \sim 38.95$ psu and $\sigma\theta \sim 29.21$ kg/m³. During a cruise in the Cretan Sea (2005), Vervatis *et al*. (2011) found a mass with core characteristics of θ 14.2°C, S 38.92 and $\sigma\theta$ 29.18kg/m³ at a depth of 750 m, which they identified as Transitional Mediterranean Water (TMW). TMW enters the Cretan Sea through the adjacent Levantine basin presenting a local salinity minimum below the LIW/CIW layers. As the time series sensor is deployed deeper than 750 m, it represents a layer influenced by the overlying TMW core and the deeper, more saline and denser Cretan masses, which at depths of more than 2000 m are denser than 29.3 kg/m³ (Vervatis *et al*., 2011).

Eastern Ionian Sea (Pylos)

Temperature and salinity data from the Pylos monitoring buoy covering a period from January 2008 to January 2011 are presented in this section. The values are shown at 1, 20, 50, 75, 100, 250, 400, and 500 m for θ and 20, 50, 75, 100, 250, 400, and 500 m for salinity as

12

Medit. Mar. Sci., SPECIAL ISSUE, 2013, 5-18
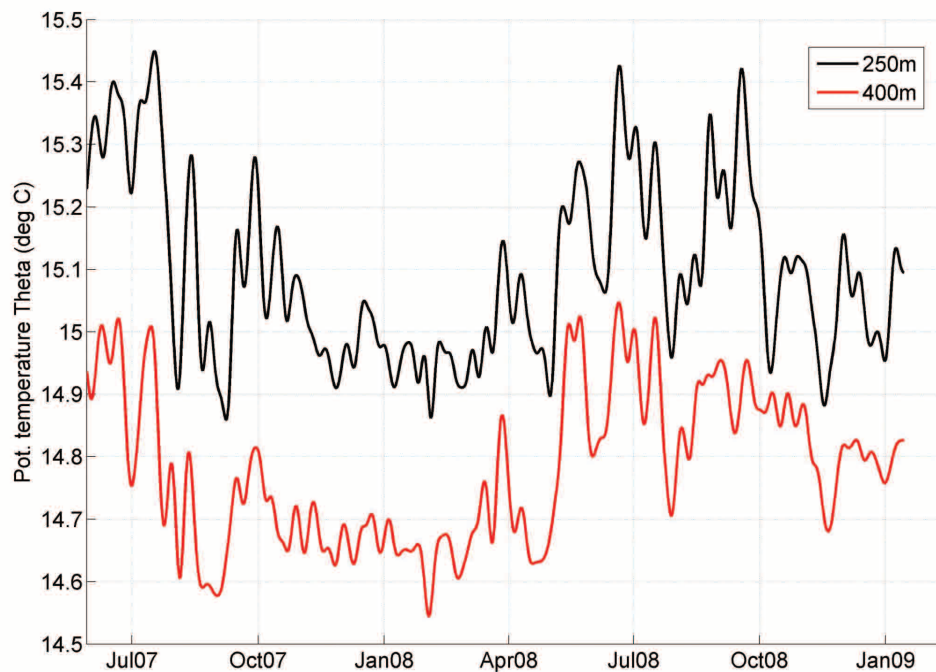
Fig. 12: Cretan Sea (E1M3A) station. Time series of potential temperature (θ) at 250 and 400 m depth (May 2007–January 2009).

again the surface salinity sensor suffers from biofouling. Again, σ_θ has been derived from valid t and S pairs only. θ, S and σ_θ time series are presented in Figures 15, 16 and 17. Figure 16 presents salinity by depth evolution instead of salinity time series at discrete depths, as the latter was hardly readable.

Surface layers

Upper layer temperature presents intense seasonal variability. The seasonal thermocline starts developing in April and peaks at the end of the summer season. The slow erosion of the thermocline starts in mid-autumn and the water column gradually becomes homogenized, due to atmospheric cooling. Homogenization reaches a cli-
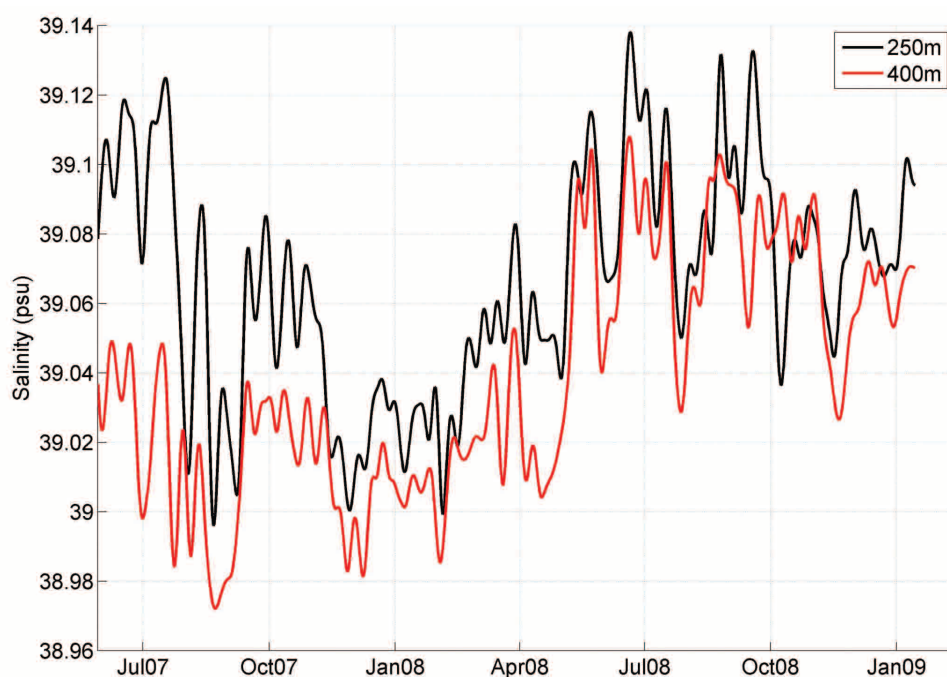
***Fig. 13:*** Cretan Sea (E1M3A) station. Time series of salinity at 250 and 400 m depth (May 2007–January 2009).
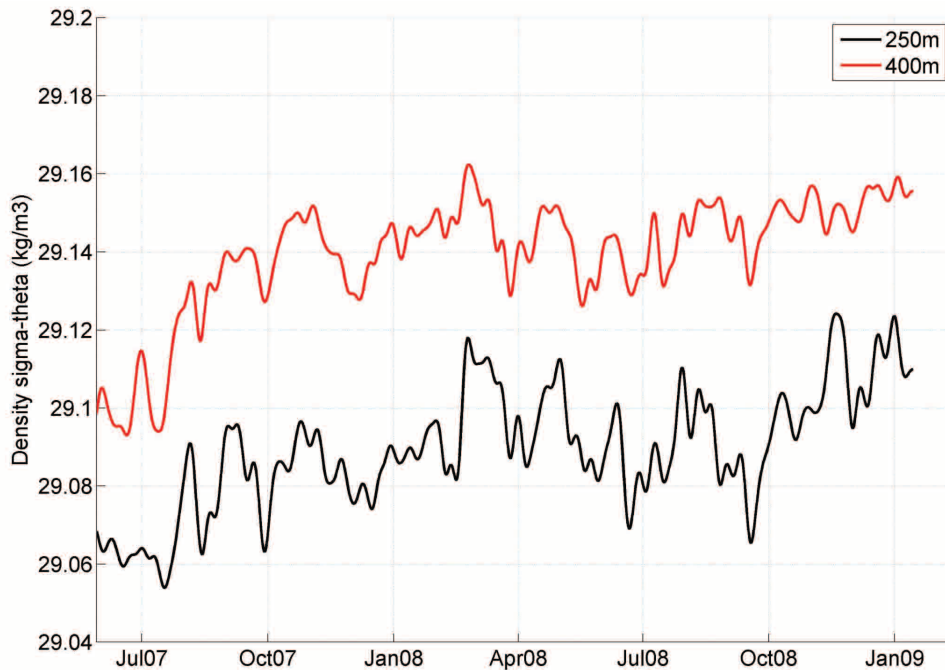
Fig. 14: Cretan Sea (E1M3A) station. Time series of potential density (σ_θ) at 250 and 400 m depth (May 2007–January 2009).

max during March and occupies the first 100 m without affecting the 250 m depth.

Low salinity (<38.8 psu) AW occupies the surface layer. This is better defined during the warm season when the AW is present down to 100 m in depth (2008, 2009). During the cold season, the AW signal is suppressed by vertical homogenization.

Intermediate layer

Figures 18, 19 and 20 present θ, S and σ_θ time series at 250 and 400 m depth. Although the time series cover only a 3-year period, a significant interannual change can be observed in the intermediate layer. A strong, warm and highly saline intermediate signal appears during spring 2009, which is enhanced during 2010 (Figures 16 and 19). This layer occupies the 100 to 500 m depth. In the
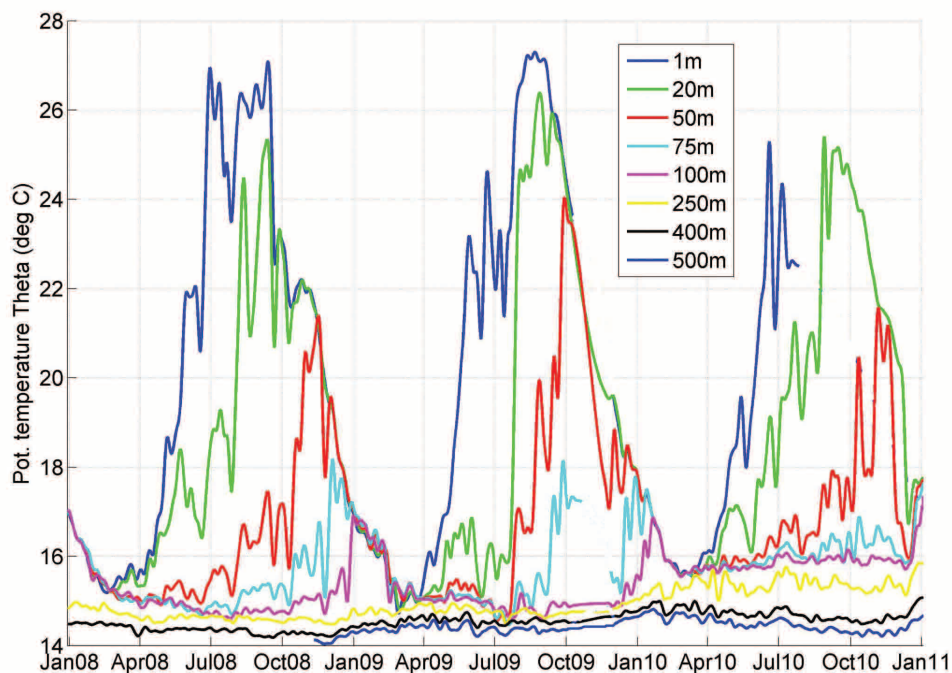
Fig. 15: Pylos station. Time series of potential temperature (θ) at 1, 20, 50, 75, 100,250, 400 and 600 m depth (January 2008–January 2011).

14

*Medit. Mar. Sci., SPECIAL ISSUE, 2013, 5-18*
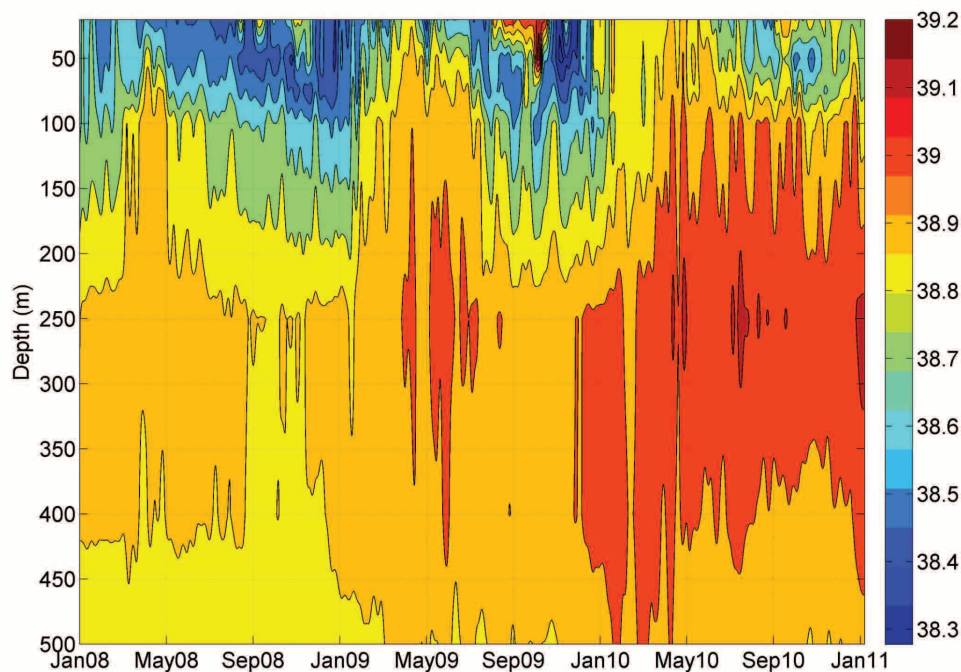
Fig. 16: Pylos station. Salinity by depth evolution (January 2008–January 2011).

warm period of 2010, its presence restricts the AW surface layer to a depth of less than 100 m. The main characteristics of this change is increased salinity at intermediate depths (~0.2 psu at 250 m) followed by increased temperature (>0.7 °C at 250 m). The salinity increase is counteracted by the temperature increase and, therefore, density appears reduced (~0.1 kg/m³).

This warm and saline intermediate mass may have originated in the Cretan Sea (increased CIW produc-

tion) and reached the South-eastern Ionian (Pylos) area through the Western Cretan Straits, or may signify an altered, more saline LIW mass. In any case, this event is an important interannual thermohaline variation that may influence Eastern Mediterranean mechanisms. For example, according to Theocharis *et al*. (2002), increased salinities in the South Ionian Sea can have an impact on water formation processes in the Adriatic Sea.
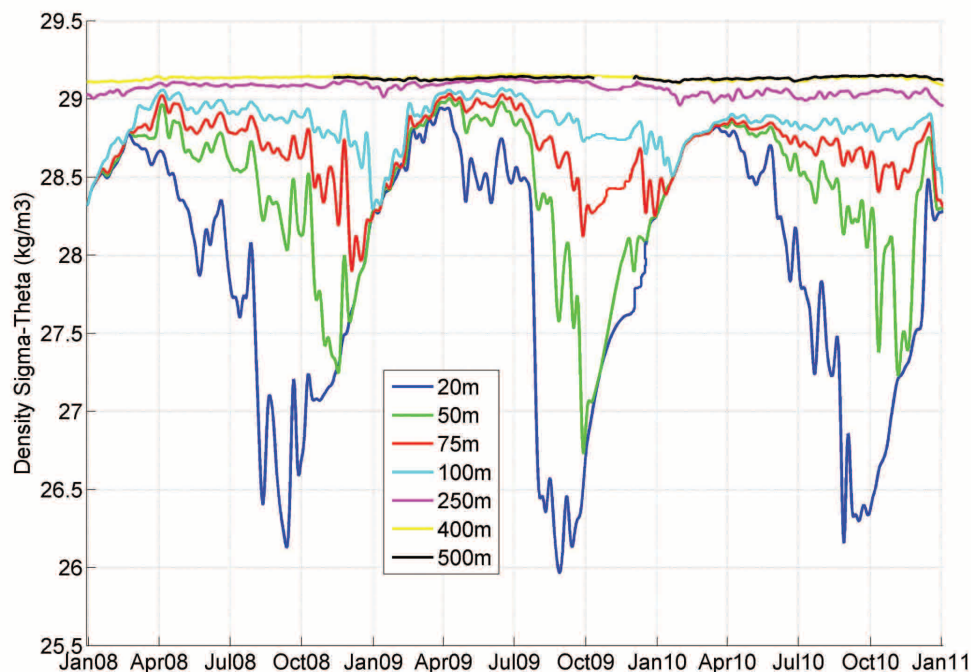
Fig. 17: Pylos station. Time series of potential density (σ_θ) at 20, 50, 75, 100,250, 400 and 600 m depth (January 2008–January 2011).

Medit. Mar. Sci., SPECIAL ISSUE, 2013, 5-18

15
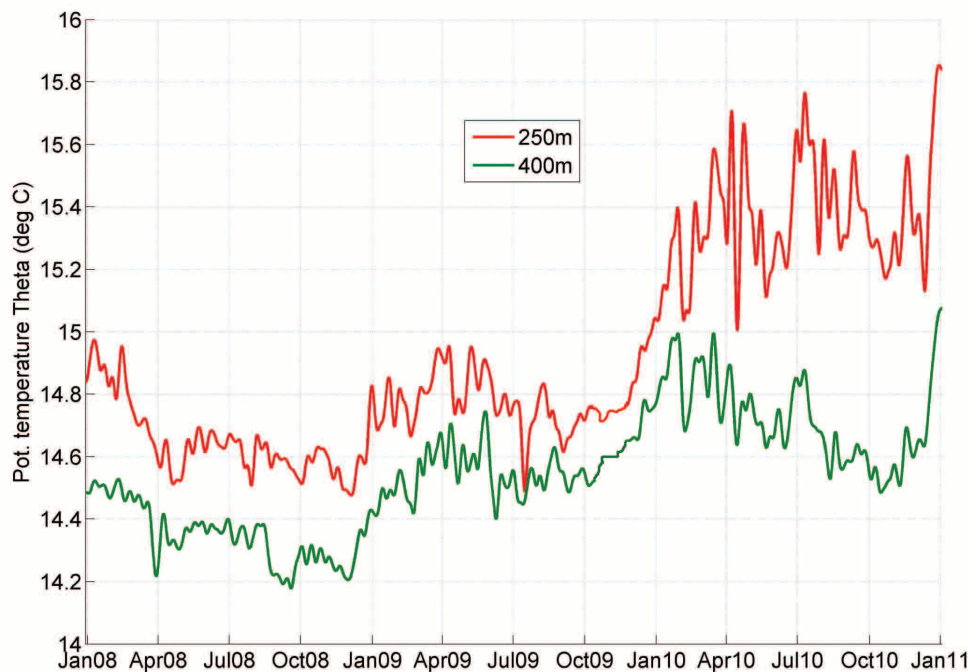
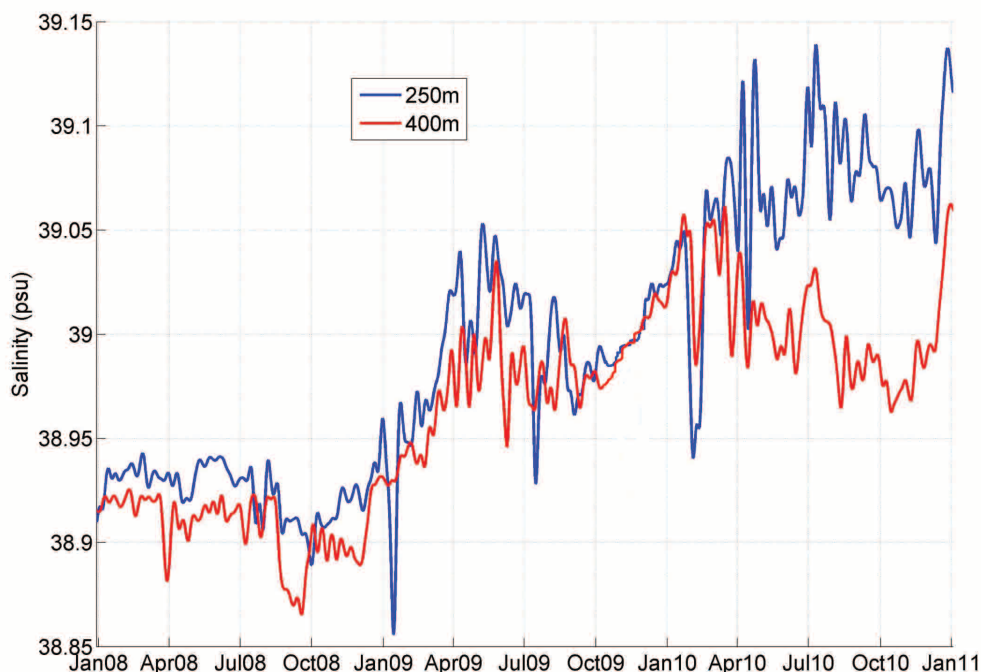**Fig. 18:** Pylos station. Time series of potential temperature (θ) at 250 and 400 m depth (January 2008–January 2011).

Conclusions

The preliminary results from the study of temperature and salinity data obtained from three POSEIDON monitoring stations presented herein reveal quite clearly the characteristics of surface and intermediate water masses in the respective areas for the particular time periods.

At the North Aegean site (Athos), low salinity surface BSW during the time range examined does not allow

winter convection to exceed the depth of 100 m. Even if the surface layer gets cold enough during winter (surface temperatures 12–13⁰ C), its low salinity restricts density to values of no more than σ_θ 29 kg/m³. During summer, density at the top of the intermediate layer (100 m) is quite high ($\sigma\theta$ ~29.2 kg/m³), much higher than that observed at the same depth during winter. Following this, it can be assumed that during the time range examined, intermediate water masses were not formed in this area where low

Fig. 19: Pylos station. Time series of salinity at 250 and 400 m depth (January 2008–January 2011).

16

Medit. Mar. Sci., SPECIAL ISSUE, 2013, 5-18

Fig. 20: Pylos station. Time series of potential density (σ_θ) at 250 and 400 m depth (January 2008–January 2011).

density BSW dominates the surface. On the other hand, in the Central Cretan Sea CIW production seems to be quite a frequent process. During the time range examined, winter convection in the buoy area penetrated at least the first 250 m. Winter convection in the Pylos buoy area did not affect more than the first 100 m. During the winter period of the examined time range no deep water formation was observed at any of the observation sites.

The observed intermediate layer temperature and salinity increase in the Central Cretan Sea after the mid-2008, cannot easily be connected to the observed temperature and salinity increase in the intermediate layer of the Eastern Ionian (Pylos) area. This is because the latter is much more intense and follows the former by more than a year. Unfortunately, the data time range is not adequate to provide information about the evolution of this increase in the Central Cretan Sea after January 2009. Additionally, it should be noted that the salinity of the intermediate layer in the Central Cretan Sea appears constantly higher than that of the same layer in the Eastern Ionian area. Nonetheless, it is possible that the observed intermediate layer temperature and salinity increase may have originated in the Cretan Sea and was then exported to the Eastern Ionian and/or it may be linked to the presence of LIW with enhanced salinity in both the Cretan and Eastern Ionian Seas.

In order to answer these issues, much more comprehensive Time series from POSEIDON monitoring stations are needed in conjunction, of course, with data from other available sources. Nevertheless, it remains clear that fixed monitoring stations play a crucial rolke in locating and interpreting large scale interannual changes.

References

Astraldi, M., Balopoulos, S., Candela, J., Font, J., Gacic, M. *et al.,* 1999. The role of straits and channels in understanding the characteristics of Mediterranean circulation. *Progress in Oceanography*, 44, 65-108.

Georgopoulos, D., Theocharis, A., Zodiatis, G., 1989. Intermediate water formation in the Cretan Sea (South Aegean Sea). *Oceanologica Acta*, 12 (4), 353-359.

Georgopoulos, D., Salusti, E., Theocharis, A., 1992. Deep water formation in the N. Aegean Sea. *Ocean Modelling*, 95, 4-6.

Gertman, I., Pinardi, N., Popov, Y., Hecht, A., 2006. Aegean Sea Water Masses during the Early Stages of the Eastern Mediterranean Climatic Transient (1988-90). *Journal of Physical Oceanography*, 36, 1841-1859.

Kress, N., Manca, B.B., Klein, B., Deponte, D., 2003. Continuing influence of the changed thermohaline circulation in the eastern Mediterranean on the distribution of dissolved oxygen and nutrients: Physical and chemical characterization of the water masses. *Journal of Geophysical Research*, 108 (C9), 8109.

Malanotte-Rizzoli, P., Manca, B., D' Alcala, M., Theocharis, A., Bergamaso, A. *et al.,* 1997. A synthesis of the Ionian hydrography, circulation and water mass pathways during POEM-Phase I. *Progress in Oceanography*, 39, 153-204.

Nittis, K., Soukissian, T., Chronis, G., 2002. Operational forecasting in the Aegean Sea: The POSEIDON system. *Elsevier Oceanography Series*, 66, 211-218.

Oğuz, T., Sur, H.I., 1989. A two-layer model of water exchange through the Dardanelles Strait. *Oceanologica Acta,* 12 (1), 23-31.

Petihakis, G., Nittis, K., Ballas, D., Kassis, D., Pagonis, P. *et al.,* 2009. The POSEIDON reference time-series stations of the Eastern Mediterranean Sea. In: *Proceedings of Ocean-Obs09: Sustained Ocean Observations and Information for Society (Annex), Venice, Italy, 21-25 September 2009,* Hall,

Medit. Mar. Sci., SPECIAL ISSUE, 2013, 5-18

17

J., Harrison D.E. and Stammer, D., (Eds), ESA Publication WPP-306. doi:10.5270/OceanObs09.

Roether, W., Klein, B., Beitzel, V., Manca, B., 1998. Property distributions and transient-tracer ages in Levantine Intermediate Water in the Eastern Mediterranean. *Journal of Marine Systems,* 18, 71-87.

Schlitzer, R., Roether, W., Oster, H., Junghans, H.G., Hausmann, M. *et al.,* 1991. Chlorofluoromethane and oxygen in the Eastern Mediterranean. *Deep Sea Research Part A. Oceanographic Research Papers,* 38 (12), 1531-1551.

Soukissian, T.H., Chronis, G.T., Nittis, K., Diamanti, C., 2002. Advancement of operational oceanography in Greece: the case of the POSEIDON system. *The Global Atmosphere and Ocean System,* 8 (2-3), 93-107.

Theocharis, A., Georgopoulos, D., 1993. Dense water formation over the Samothraki and Limnos Plateaux in the north Aegean Sea (eastern Mediterranean Sea). *Continental Shelf Research*, 13 (8), 919-939.

Theocharis, A., Georgopoulos, D., Lascaratos, A., Nittis, K., 1993. Water masses and circulation in the central region of the Eastern Mediterranean: Eastern Ionian, South Aegean, and Northwest Levantine, 1986-1987. *Deep-Sea Research II*, 40, (6), 1121-1142.

Theocharis, A., Papageorgiou, E., Kontoyiannis, H., Nittis, K., Balopoulos, E., 1998. The evolution of the Aegean water's influence in the deep thermohaline circulation of the Eastern Mediterranean (1986–1995). *Rapport Commission Internationale pour l' Exploration Scientifique de la Mer Mediterranee,* 35, 200-201.

Theocharis, A., Balopoulos, E., Kioroglou, S., Kontoyiannis, H., Iona, A., 1999. A synthesis of the circulation and hydrography of the South Aegean Sea and the Straits of the Cretan Arc (March 1994-January 1995). *Progress in Oceanography,* 44, 469-509.

Theocharis A., Klein B., Nittis, K., Roether W., 2002. Evolution and status of the Eastern Mediterranean Transient (1997-1999), *Journal of Marine Systems,* (33-34), 91-116.

Unesco, 1983. Algorithms for computation of fundamental properties of seawater. Unesco technical papers in marine science (44).

Ünlüata, U., Oğuz, T., Latif, M.A., Ozsoy, E., 1990. On the physical oceanography of the Turkish Straits. p. 25-60. In: *The Physical Oceanography of Sea Straits,* L. J. Pratt (Ed.), Kluwer Academic Publishers.

Wüst, G., 1961. On the vertical circulation of the Mediterranean Sea. *Journal of Geophysical Research,* 66 (10), 3261-3271.

Velaoras, D., Lascaratos, A., 2005. Deep water mass characteristics and interannual variability in the North and Central Aegean Sea. *Journal of Marine Systems*, 53, 59-85.

Velaoras, D., Lascaratos, A., 2010. North-Central Aegean Sea surface and intermediate water masses and their role in triggering the Eastern Mediterranean Transient. *Journal of Marine Systems,* 83, 58-66.

Vervatis, V., Sofianos, S., Theocharis, A., 2011. Distribution of the thermohaline characteristics in the Aegean Sea related to water mass formation processes (2005-2006 winter surveys). *Journal of Geophysical Research,* (116), C09034.

Zervakis, V., Georgopoulos, D., Drakopoulos, P., 2000. The role of the North Aegean in triggering the recent Eastern Mediterranean climatic changes. *Journal of Geophysical Research* 105 (C11), 26103-26116.

Zervakis, V., Theocharis, A., Georgopoulos, D., 2005. Circulation and hydrography of the open seas, 104-110. In: *State of the Hellenic Marine Environment.* Papathanasiou, E. & Zenetos, A. (Eds) HCMR, Athens.

Zodiatis, G., 1991. The hydrological conditions and the circulation in the Cretan Sea during late summer 1987. Annales Geophysicae, 9, 233-238.

Zodiatis, G., 1993. Circulation of the Cretan Sea water masses (Eastern Mediterranean Sea). *Oceanologica Acta*, 16, 2, 107-114.

Zodiatis, G., 1994. Advection of the Black Sea water in the North Aegean Sea. *The Global Atmosphere and Ocean System,* 2, 41-61.

Zodiatis, G., Alexandri, S., Pavlakis, P., Jonsson, L., Kallos, G. *et al.,* 1996. Tendative study of flow patterns in the North Aegean Sea using NOAA-AVHRR images and 2D model Simulation. *Annales Geophysicae*, 14, 1221-1231.

18

Medit. Mar. Sci., SPECIAL ISSUE, 2013, 5-18